Int. J. Electrochem. Sci., 16 **(2021)** 150858, doi: 10.20964/2021.01.13

International Journal of
ELECTROCHEMICAL
SCIENCE
www.electrochemsci.org

Poly-levodopa as an Eco-friendly Corrosion Inhibitor for Q235 Steel

Feng Yang[1], *Jiayu Wei*[1,2], *Shihui Qiu*[2,*], *Chengbao Liu*[2], *Li Cheng*[2], *Haichao Zhao*[2,*]

[1] School of Materials Science and Engineering, Shenyang University of Chemical Technology, Shen Yang, 110142, China
[2] Key Laboratory of Marine Materials and Related Technologies, Zhejiang Key Laboratory of Marine Materials and Protective Technologies, Ningbo Institute of Materials Technology and Engineering, Chinese Academy of Sciences, Ningbo 315201, P. R. China.
[*]E-mail: qiushihui@nimte.ac.cn, zhaohaichao@nimte.ac.cn

Received: 21 August 2020 / *Accepted:* 2 November 2020 / *Published:* 30 November 2020

The corrosion inhibition effect of polylevodopa (poly-(L-DOPA)) on Q235 carbon steel in 1 M HCl was studied owing to its low cytotoxicity and special structure. Electrochemical measurements show that the corrosion inhibition efficiency increases with the increase of poly-(L-DOPA) concentration and the immersion time. When the concentration of poly-(L-DOPA) is 300 mg/L, the corrosion inhibition efficiency can reach 97%. Confocal laser scanning microscopy (CLSM) and field emission scanning electron microscope (FESEM) proved that poly-(L-DOPA) has a good corrosion inhibition effect on Q235 carbon steel immersed in 1 M HCl. Poly-(L-DOPA) adsorbs on the surface of Q235 carbon steel to form a protective film, and followed the Langmuir adsorption isotherm.

Keywords: Poly-(L-DOPA); Q235 Steel; Corrosion inhibition; Hydrochloric acid solution

1. INTRODUCTION

Metal is widely used in various industries as a common material and one of the basic materials for the construction industry and manufacturing industry. However, metal corrosion is a huge hazard to human society, which severely restricts the scope of application and service life of metal materials. In industry, it is very important to protect metals from being corroded by acid solutions during descaling and rust removal[1-3]. Adding corrosion inhibitors is a common method to protect metals from corrosion[4-7]. Many inorganic salts (i.e., chromates[8], polyphosphates[9] and nitrites[10]) and organic compounds are excellent corrosion inhibitors. However, the high toxicity of inorganic substances limits its application[11].

The organic corrosion inhibitor protects the metal by forming a protective film on the metal surface to prevent the reaction between the metal and the corrosive medium[12-14]. Common organic corrosion inhibitors are mostly organic heterocyclic compounds containing heteroatoms (i.e., N, O, S, P)[15-18], unsaturated bonds or polar functional groups[19-22]. Including amines (i.e., o-substituted anilines[23], aromatic amides[24], Schiff bases[25], etc.), amino acids[26] (i.e., glycine, cysteine, etc.), azoles (i.e., benzotriazole and its derivatives[25], halogenated indazole compounds[27], thiazole[28-29], imidazole and its derivatives[30-32], etc.) and dithiophosphate derivatives[33]. Because nitrogen atoms easily donate electrons to metals, nitrogen-containing compounds are most used[34]. Although these corrosion inhibitors have excellent effects, most of the organic compounds are toxic and harmful to the environment and humans[35-36].

With increasing attention to environmental protection issues, researchers have focused on the development of environmentally friendly inhibitors. It is currently known that several natural products have been used as corrosion inhibitors, including banana peel extract, longan seed and pericarp extract[37], white calamus peel extract[38], red algae extract[39], ginkgo biloba extract[40], etc. At the same time, some drugs[41-43] have natural sources and are non-toxic, and they are also considered to be ideal "green" corrosion inhibitors.

Levodopa (3-(3, 4-Dihydroxyphenyl)-L-alanine, L-DOPA) is one of the precursors for the synthesis of norepinephrine and dopamine (DA) in humans and animals. Since DA was reported to be used as an adhesive material to modify the surface of a variety of materials[44], more and more researches have focused on the application of DA's precursor L-DOPA in the field of materials. L-DOPA can be easily polymerized in alkaline environment, and the structure contains electronegative atoms and multiple chemical bonds, including amino, carboxyl, hydroxyl and other functional groups. At the same time, DA has also been reported as an effective corrosion inhibitor for the corrosion of low carbon steel in 1 M HCl[45]. It is expected that it can act as an environmentally friendly corrosion inhibitor to inhibit metal corrosion.

In the current work, we have prepared polylevodopa in an alkaline environment and investigated its corrosion inhibition effect. Through electrochemical polarization and impedance testing, FESEM and CLSM to research the corrosion inhibition effect in 1 M HCl solution.

2. EXPERIMENTAL

2.1. Materials

Levodopa (L-DOPA) used in this study was purchased from Aladdin Industries. Sodium hydroxide, ethanol and hydrochloric acid (36%-38%) were purchased from Sinopharm Chemical Reagent Co., Ltd. (Shanghai, China). 10×10×10 mm^3 and 10×10×1 mm^3 Q235 carbon steel were purchased from Shengxin Technology Co., Ltd. Deionized water (DI) was used throughout the experiment.

2.2. Synthesis of poly-(L-DOPA)

The synthetic route of poly-(L-DOPA) is shown in Scheme 1. First of all, 0.5 g of sodium hydroxide is dissolved in 100 ml of deionized water, and after it is completely dissolved, 2.46 g of levodopa is added to it. Stir slowly and react at room temperature for 24 hours to obtain a dark brown solution. After the reaction, the liquid was freeze-dried to obtain a black solid.

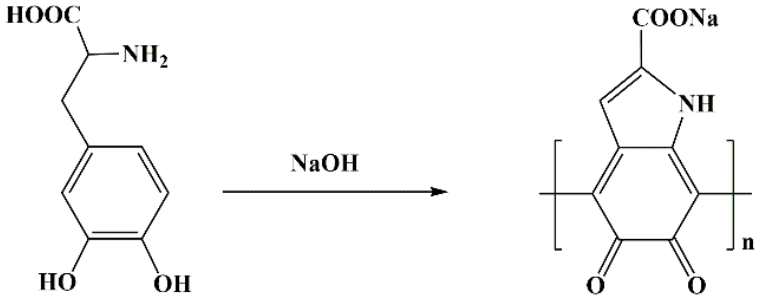

Scheme 1. The synthesis of the poly-(L-DOPA).

2.3. Preparation of electrodes and solutions

The Q235 carbon steel is ultrasonically cleaned with alcohol, degreased and dried. Sealed with epoxy resin, the test area is 1 cm^2. Before the test, use 150, 400, 800, and 1200 mesh SiC sandpaper for polishing.

Dilute AR grade 36%-38% HCl with DI to prepare 1 M HCl solution. Poly-(L-DOPA) is added to it to configure different concentrations of corrosive liquid. Each test uses a freshly prepared solution.

2.4. Characterization of poly-(L-DOPA)

Fourier transform infrared (FT-IR) spectrum was obtained on Nicolet 6700 FT-IR spectrometer. A Lambda 950 spectroscope was used to record the ultraviolet-visible absorption spectrum (UV-vis) spectrum between 300-800 nm. After immersing Q235 carbon steel in 1 M HCl solution containing different concentrations of poly-(L-DOPA) for 12 hours, the surface morphology of the sample was recorded on the FEI Quanta FEG 250 field emission scanning electron microscope (FESEM). Similarly, a laser confocal microscope (Zeiss) LSM 700 was used to record the roughness of the sample surface.

2.5. Electrochemical measurement

The electrochemical measurement was recorded on Shanghai Chenhua CHI-660E electrochemical workstation. Electrochemical impedance and polarization tests were carried out in an ordinary three-electrode battery with platinum foil as the counter electrode and saturated calomel electrode as the reference electrode. Q235 carbon steel with a working area of 1 cm^2 is the working electrode. All tests are performed at room temperature. The electrochemical test is performed after the

open circuit potential (OCP) has stabilized. Electrochemical impedance spectroscopy (EIS) measurements are performed in the frequency range of 100 kHz to 10 mHz and use Zsimpwin 3.21 software to fit and analyze. Finally, a potentiodynamic polarization test was carried out relative to OCP within a potential range of ±300 mV, with a scan rate of 0.01 V/s, and the same test was performed 3 times to ensure reliability.

Calculate the corrosion inhibition efficiency (η) and surface coverage (θ) according to the following formula through the polarization curve.

$$\eta = \frac{i^0_{corr} - i_{corr}}{i^0_{corr}} \times 100 \cdots\cdots\cdots\cdots\cdots\cdots\cdots\cdots\cdots\cdots (1)$$

$$\theta = \frac{i^0_{corr} - i_{corr}}{i^0_{corr}} \cdots\cdots\cdots\cdots\cdots\cdots\cdots\cdots\cdots\cdots (2)$$

Where i_{corr} and i^0_{corr} represent the corrosion current density in the presence and absence of inhibitors.

Use ZsimpWin software to fit the EIS data, and use the following formula to calculate the corrosion inhibitor efficiency IE% according to the fitting results.

$$IE\% = \frac{R_{ct} - R^0_{ct}}{R_{ct}} \times 100\% \cdots\cdots\cdots\cdots\cdots\cdots\cdots (3)$$

Where R_{ct} and R^0_{ct} represent the charge transfer resistance in the presence and absence of inhibitor.

2.6. Adsorption isotherm

The adsorption isotherm curve is one of the most effective methods to study the adsorption of corrosion inhibitor layers on organic inhibitors and metal surfaces[46-47]. The Langmuir adsorption isotherm is considered to be suitable for fitting the results obtained by EIS and is given by the following equation:

$$\frac{C_{inh}}{\theta} = \frac{1}{K_{ads}} + C_{inh} \cdots\cdots\cdots\cdots\cdots\cdots\cdots\cdots\cdots (4)$$

In the equation, C_{inh} is the concentration of corrosion inhibitor, and K_{ads} is the equilibrium constant of the adsorption-desorption process. The intercept between C_{inh} and C_{inh}/θ is $1/K_{ads}$.

The standard free energy of adsorption (ΔG_{ads}) can be obtained by the following formula:

$$K_{ads} = \frac{1}{55.5} \exp\left(-\frac{\Delta G_{ads}}{RT}\right) \cdots\cdots\cdots\cdots\cdots\cdots (5)$$

In the formula, R is the gas constant, T is the absolute temperature (K), 55.5 is the concentration of water in the solution, and the unit is mol/L.

3. RESULTS AND DISCUSSION

3.1. Synthesis and characterization of poly-(L-DOPA)

The FT-IR spectrum of poly-(L-DOPA) is shown in Figure 1. The absorption peak at 3330 cm^{-1} is the stretching vibration of the N-H bond. The absorption peak at 1586 cm^{-1} is attributed to the bending

vibration of N-H[45]. The stretching vibration of C-N is located at 1390 cm^{-1}. Since the N atom does not share an electron pair to conjugate with the carbonyl group P-π, the C-N bond moves in the direction of high wavenumber. The broad and scattered absorption peak at 650 cm^{-1} is the out-of-plane bending vibration of the N-H bond[48].

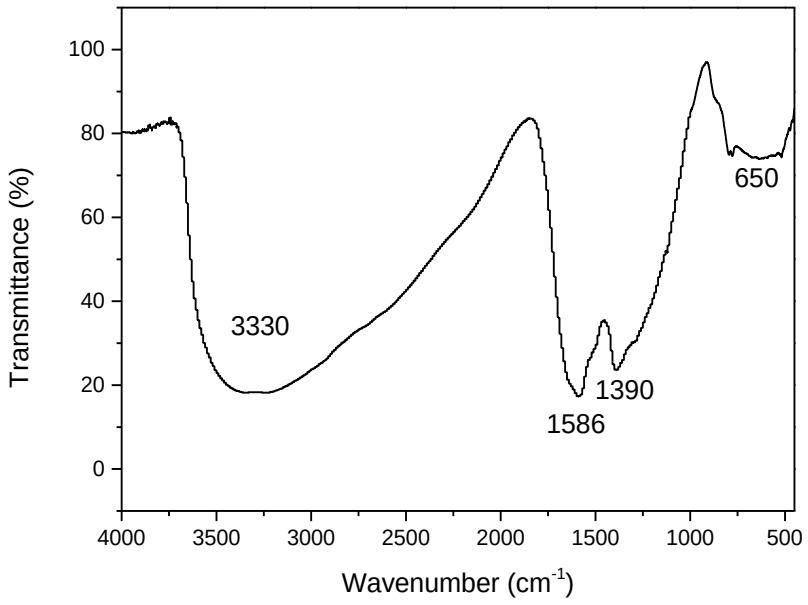

Figure 1. The FT-IR spectrum of poly-(L-DOPA).

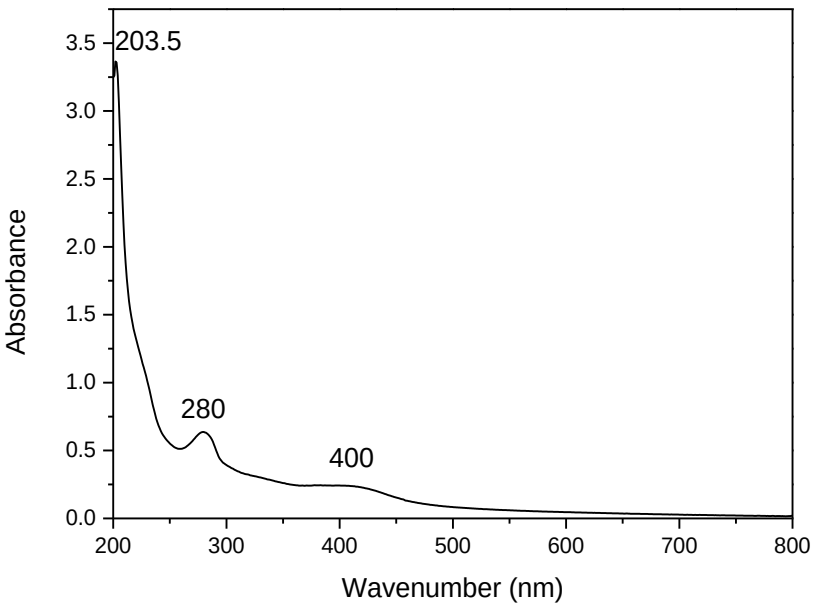

Figure 2. UV-vis absorption spectrum of poly-(L-DOPA).

Figure 2 shows the UV-vis absorption spectrum of poly-(L-DOPA). The absorption peak at 203.5 nm is the π-π* transition caused by benzene ring conjugated diene, and the absorption peak at 280 nm is caused by the benzene ring vibration and π-π* overlap. The absorption peak near 400 nm is the n-π*

transition of the benzene ring on the polymer backbone, which is a typical absorption peak of the o-quinone family[49].

3.2. Polarization measurements

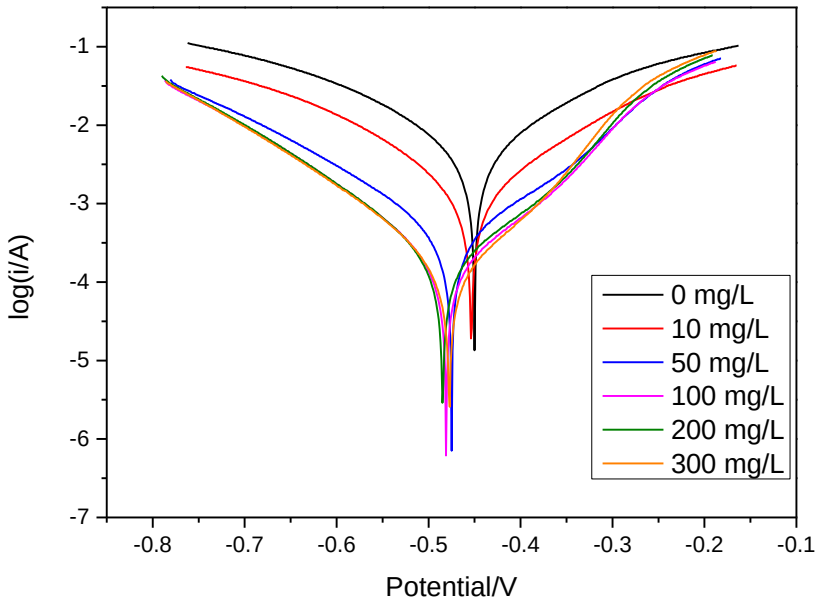

Figure 3. Polarization curves of Q235 carbon steel in 1 M HCl solution containing different concentrations of poly-(L-DOPA).

Table 1. Electrochemical parameters obtained by polarization curves of Q235 carbon steel in 1 M HCl solution containing different concentrations of poly-(L-DOPA)

Samples	E_{corr} (mV)	i_{corr} (10^{-5} A cm^{-2})	β_a (mV/dec)	β_c (mV/dec)	θ	η
0 mg/L	-450	383.35	145	-150	-	-
10 mg/L	-454	124.74	141	-133	0.6746	67.46%
50 mg/L	-475	30.70	133	-121	0.9199	91.99%
100 mg/L	-482	13.55	109	-94	0.9647	96.47%
200 mg/L	-486	12.96	114	-95	0.9662	96.62%
300 mg/L	-477	8.38	88	-82	0.9781	97.81%

Figure 3 shows the polarization curves of Q235 carbon steel after soaking in 1 M HCl solution containing different concentrations of poly-(L-DOPA) for 12 hours. Table 1 lists the electrochemical parameters obtained by measuring the polarization curve, including corrosion potential (E_{corr}), corrosion current density (i_{corr}), cathode Tafel slope (β_c), anode Tafel slope (β_a), surface coverage (θ) and corrosion inhibition efficiency (η). It can be observed that as the concentration of poly-(L-DOPA) increases, the polarization pattern shifts to a negative potential. The i_{corr} decreases with the increase of poly-(L-DOPA) concentration, which can be attributed to the adsorption layer formed on the surface of Q235 carbon steel, which limits the diffusion of oxygen from the solution to the cathode of Q235 carbon steel[50]. At

the same time, the value of η also increases with the increase of poly-(L-DOPA) concentration. When the concentration of poly-(L-DOPA) is 100 mg/L, the inhibition efficiency can reach 96%. It can be considered that poly-(L-DOPA) is an effective corrosion inhibitor for Q235 carbon steel in 1 M HCl solution. In addition, the values of β_c and β_a also change with the addition of poly-(L-DOPA), indicating that poly-(L-DOPA) has an inhibitory effect on both anode and cathode reactions, and the corrosion inhibitor is a mixed inhibitor[51].

3.3. Electrochemical impedance spectroscopy

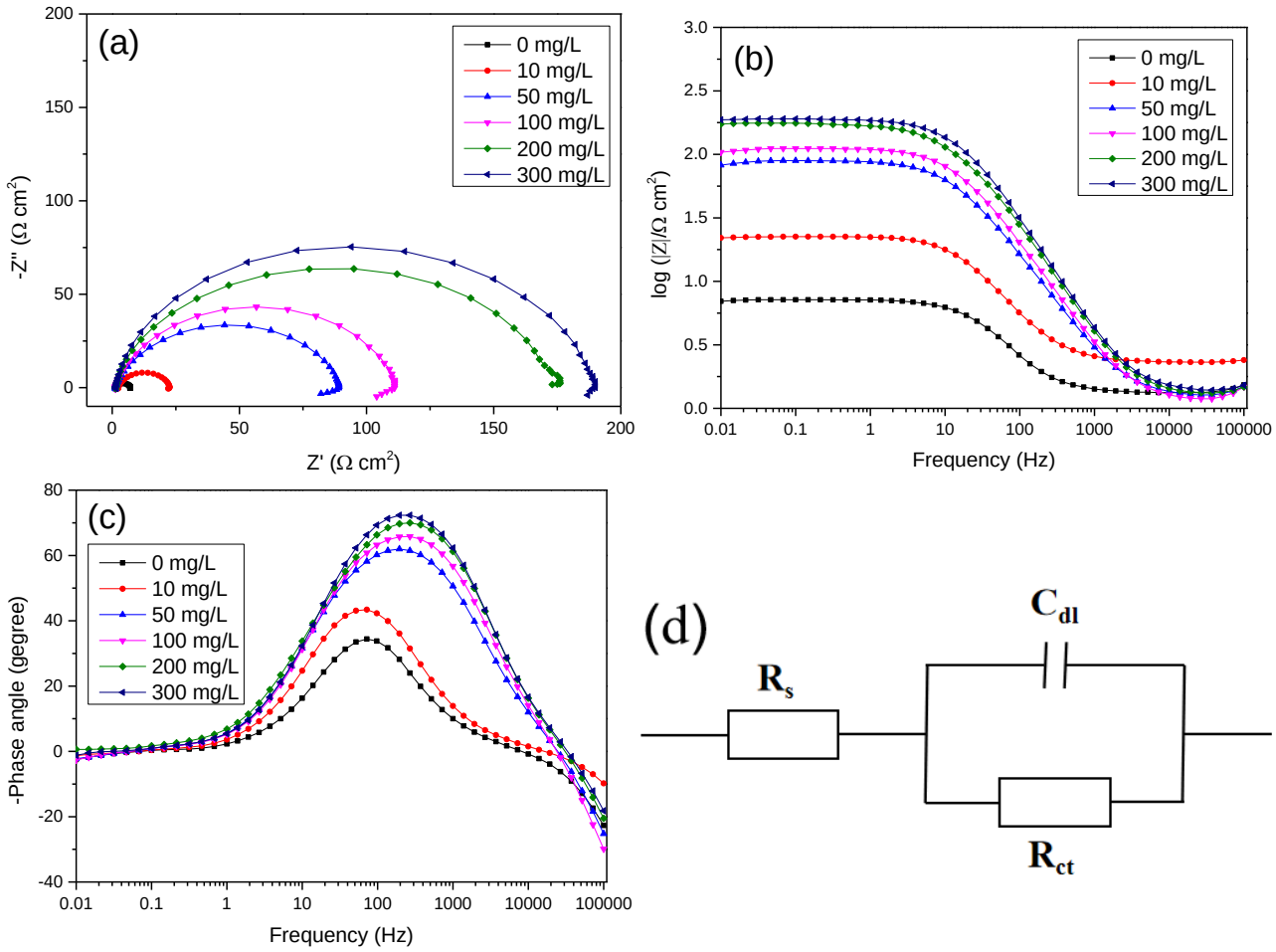

Figure 4. Nyquist (a) and Bode (b and c) graphs of Q235 carbon steel immersed in 1 M HCl solution containing different concentrations of poly-(L-DOPA) for 12 hours, and the equivalent circuit (d) is used to fit the EIS results.

Electrochemical impedance spectroscopy measures the impedance change with the frequency of the sine wave, and then analyzes the electrode process dynamics, adsorption and diffusion, and corrosion protection mechanism. Figure 4 shows the Nyquist (a) and Bode (b and c) diagrams of Q235 carbon steel immersed in 1 M HCl solution containing different concentrations of poly-(L-DOPA) for 12 hours. The ZSimpwin software was used to perform the fitting through the equivalent circuit in Figure 4(d), and the fitting parameters are listed in Table 2. In the equivalent circuit, R_s is the solution resistance, C_{dl}

is the double-layer capacitor, and R_{ct} is the charge transfer resistance. The corrosion inhibitor efficiency (IE%) is calculated.

Table 2. Fitting parameters of Q235 carbon steel immersed in 1 M HCl solution containing different concentrations of poly-(L-DOPA) for 12 hours.

Samples	R_s (Ω cm^2)	C_{dl} (F cm^{-2})	R_{ct} (Ω cm^2)	IE%
0 mg/L	1.37	1.92×10^{-3}	5.76	-
10 mg/L	2.33	9.01×10^{-4}	20.26	71.59
50 mg/L	1.34	2.50×10^{-4}	86.79	93.37
100 mg/L	1.28	1.66×10^{-4}	108.20	94.68
200 mg/L	1.35	1.20×10^{-4}	169.40	96.60
300 mg/L	1.43	8.78×10^{-5}	185.00	96.89

All EIS plots in Figure 4 show similar shapes, indicating the addition of poly-(L-DOPA) did not change the electrochemical properties of the solution. The capacitive loop in the Nyquist diagram is slightly concave, and the center of the circle is below the solid axis. This may be the charge transfer process when the carbon steel is dissolved, or it may be related to the surface roughness of the carbon steel and the adsorption of inhibitors[40]. The diameter of the capacitor ring increases with the increase of poly-(L-DOPA) concentration, which indicates that more and more inhibitor molecules are adsorbed on the surface of Q235 carbon steel, and the protective film becomes denser[52-53]. Figure 4b shows the Bode impedance diagram. Usually, the impedance value at low frequency can reflect the corrosion inhibition ability of the sample. It can be observed from Figure 4b that as the concentration of poly-(L-DOPA) increases, the impedance value at low frequencies gradually increases. This shows that poly-(L-DOPA) has a good corrosion inhibition effect. The higher the concentration, the slower the corrosion process and the higher the corrosion inhibition efficiency[54]. It can be seen from the Bode phase angle diagram of Figure 4c that poly-(L-DOPA) exhibits a good corrosion inhibition effect at high frequencies.

It can be seen from the data in Table 2, as the concentration of poly-(L-DOPA) increases, the charge transfer resistance R_{ct} gradually increases, and the double-layer capacitance C_{dl} gradually decreases. The increase in R_{ct} and the decrease in C_{dl} can be attributed to the formation of a protective layer on the metal surface, thereby reducing the charge transfer between the metal surface and the electrolyte[55]. When poly-(L-DOPA) concentration is 50 mg/L, IE% can reach 93.37%. These results show that the addition of poly-(L-DOPA) has corrosion inhibition ability for Q235 carbon steel immersed in 1 M HCl.

3.4. Adsorption isotherm

Through the adsorption isotherm, we can understand the interaction between poly-(L-DOPA) and Q235 carbon steel surface and the adsorption performance of the adsorbent[55]. As shown in Figure 5, plotting the relationship between inhibitor concentration C_{inh} and C_{inh}/θ, a straight line with an intercept of $1/K_{ads}$ can be obtained, indicating that the adsorption of poly-(L-DOPA) on the surface of

Q235 carbon steel obeys the Langmuir adsorption isotherm. The equilibrium constant k_{ads} is obtained from the adsorption isotherm, and the standard free energy (ΔG_{ads}) is calculated using formula (4). Generally speaking, ΔG_{ads} can be used to understand the adsorption type of corrosion inhibitor. When ΔG_{ads} is greater than -20 kJ/mol, it is physical adsorption, and when ΔG_{ads} is less than -40 kJ/mol, it is chemical adsorption[56]. The calculated value of ΔGads in present work is -31.2 kJ/mol, which is physical adsorption and chemical adsorption, and there is electrostatic interaction between poly-(L-DOPA) and the surface of Q235 carbon steel. A higher K_{ads} value indicates that the inhibitor can be closely adsorbed on the metal surface to form a dense protective film[57].

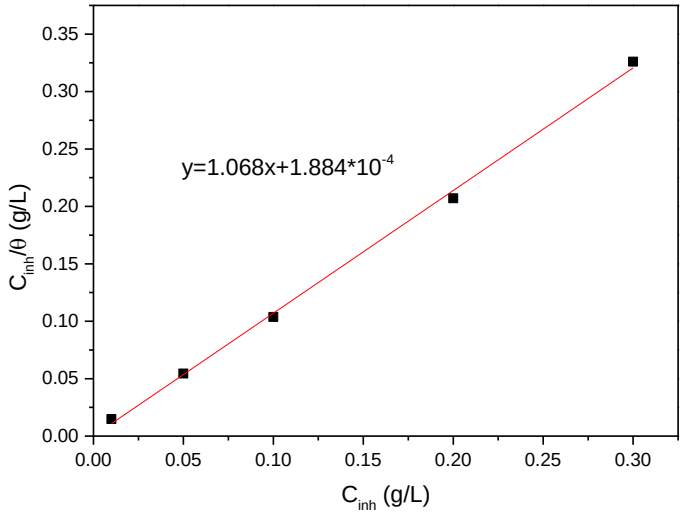

Figure 5. Langmuir adsorption isotherms on the surface of Q235 carbon steel in 1 M HCl solution

3.5. Influence of immersion time

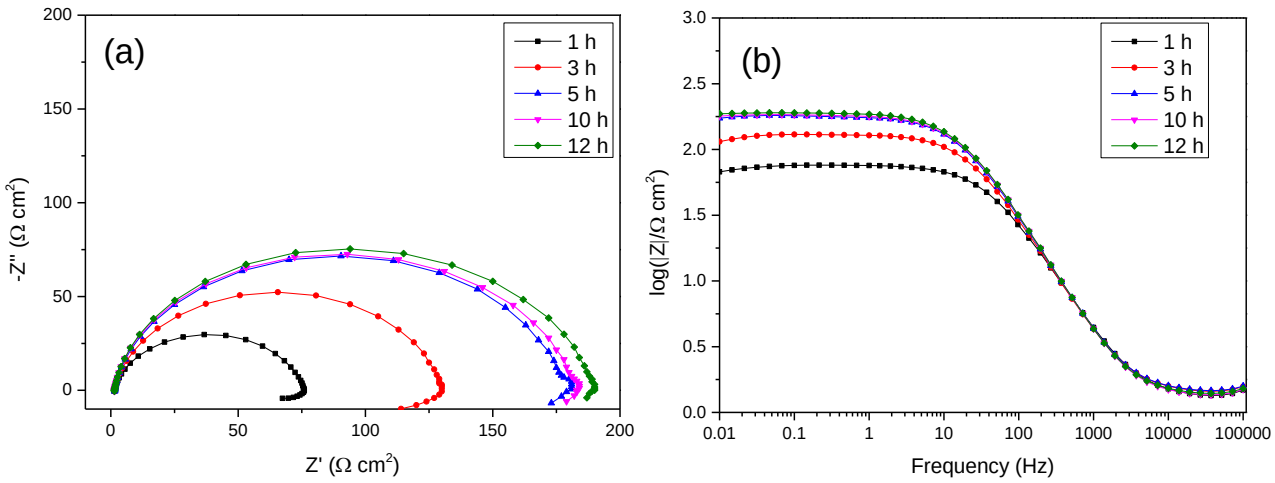

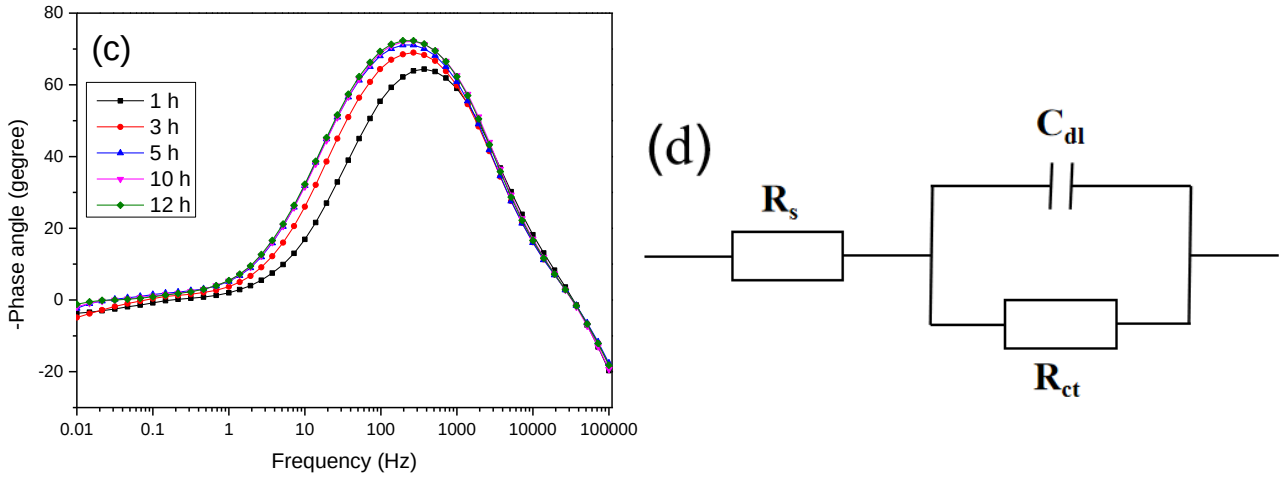

Figure 6. Nyquist (a) and Bode (b and c) diagrams of Q235 carbon steel immersed in 1 M HCl solution containing 300 mg/L poly-(L-DOPA) for different time, and fitted the EIS result with the equivalent circuit (d) .

Table 3. Fitting parameters of Q235 carbon steel immersed in 1 M HCl solution containing 300 mg/L poly-(L-DOPA) for different time.

Time	R_s (Ω cm^2)	C_{dl} (F cm^{-2})	R_{ct} (Ω cm^2)
1 h	1.39	1.07×10^{-4}	72.91
3 h	1.49	9.81×10^{-5}	125.70
5 h	1.50	9.41×10^{-5}	175.20
10 h	1.40	8.84×10^{-5}	178.40
12 h	1.43	8.78×10^{-5}	185.00

In order to research the effect of time on the corrosion behavior of Q235 carbon steel immersed in 1 M HCl with poly-(L-DOPA), a long-term EIS test was used. We choose 1 M HCl solution containing 300 mg/L poly-(L-DOPA) as the research object of EIS.

Figure 6 shows the Nyquist (a) and Bode (b and c) graphs of Q235 carbon steel immersed in a 1 M HCl solution containing 300 mg/L poly-(L-DOPA) for different times. It can be seen from the Nyquist graph that, as the immersion time increases, the diameter and impedance of the capacitor ring at low frequencies also increase, which indicates that the corrosion inhibitor has an enhanced inhibitory effect on the corrosion of Q235 carbon steel. Figure 6b shows the Bode impedance diagram. At low frequencies, the impedance value increases with time, and the corrosion inhibition efficiency gradually increases, showing good corrosion inhibition. When the immersion time reaches 5 h, the corrosion inhibition efficiency does not change much. Fit the equivalent circuit in Figure 6d, and the results are listed in Table 3. Obviously, as the immersion time increases, the double-layer capacitance C_{dl} gradually decreases, the charge transfer resistance R_{ct} gradually increases, and the corrosion inhibition efficiency gradually increases[58].

3.6. Surface analysis

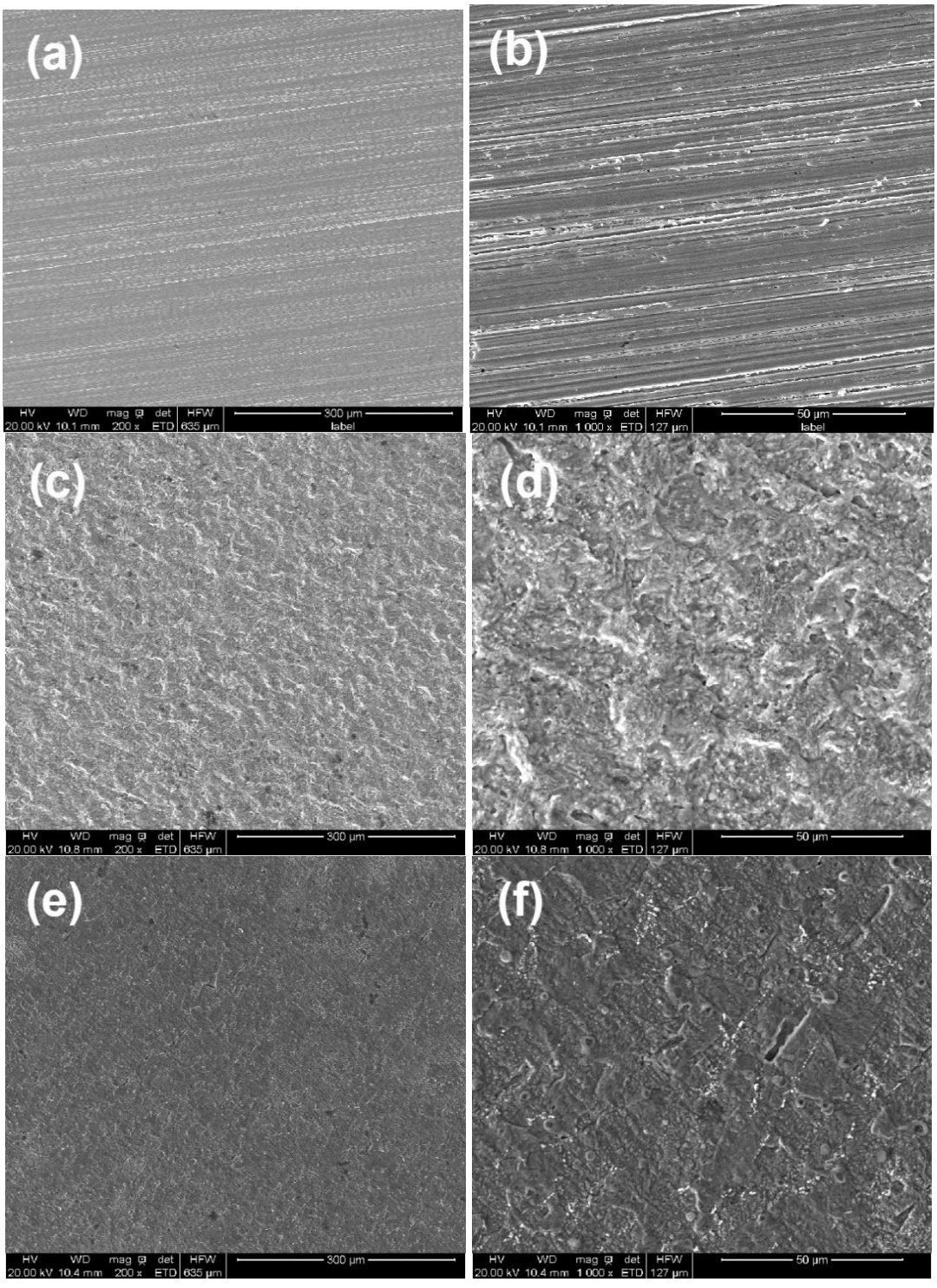

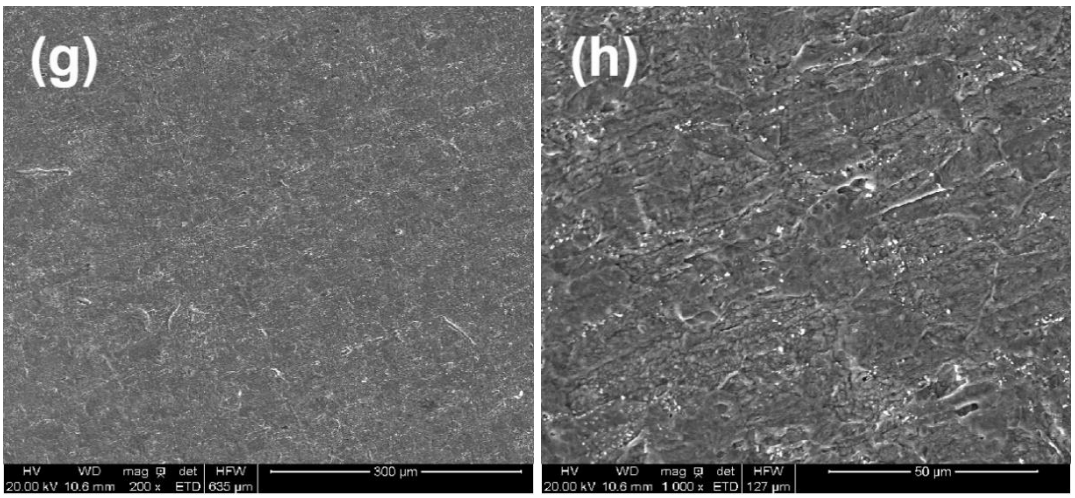

Figure 7. SEM images of Q235 carbon steel after polishing (a-b) and immersed in 1 M HCl solution containing different concentrations of poly-(L-DOPA) for 12 hours (0 mg/L poly-(L-DOPA) (c-d), 50 mg/L poly-(L-DOPA) (e-f) and 300 mg/L poly-(L-DOPA) (g-h)).

Figure 7 shows the SEM image of 10×10×1 mm^3 Q235 carbon steel immersed in 1 M HCl solution containing different concentrations of poly-(L-DOPA) for 12 hours.

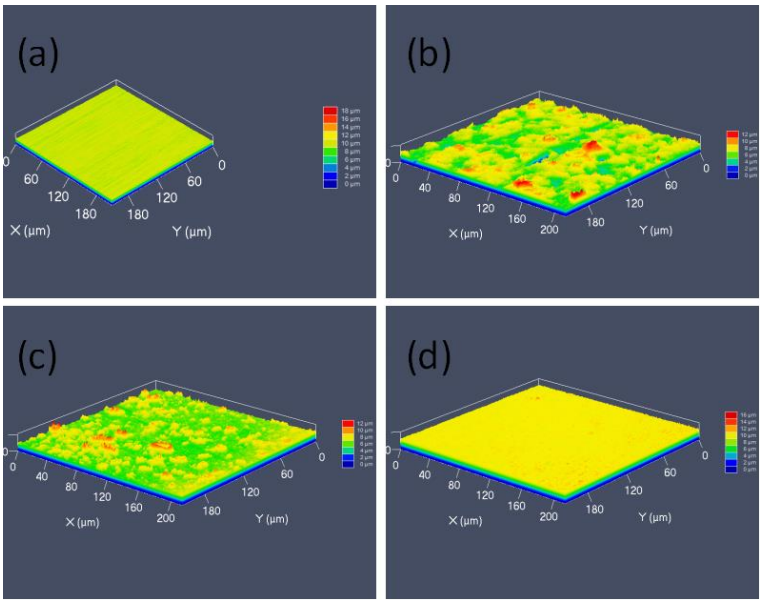

Figure 8. CLSM images of Q235 carbon steel after polishing (a) and immersed in 1 M HCl solution containing different concentrations of poly-(L-DOPA) for 12h (0 mg/L poly-(L-DOPA) (b), 50 mg/L poly-(L-DOPA) (c) and 300 mg/L poly-(L-DOPA) (d)).

It can be seen from Figure 7a-b that the polished Q235 carbon steel has a smooth surface, with scratches caused by polishing and no obvious defects. Figure 7c-d shows the surface morphology of Q235 carbon steel after immersing in 1 M HCl. It can be seen that there are pits and cracks on the surface of Q235 carbon steel, which are severely corroded[59]. However, when poly-(L-DOPA) is present in

the solution (Figure 7e-f), the corrosion of the sample surface is reduced. This is because poly-(L-DOPA) is adsorbed on the surface of Q235 carbon steel, reducing the corrosion rate. When the concentration of poly-(L-DOPA) is 300 mg/L (Figure 7g-h), it shows a good inhibitory effect. The surface of the sample is smooth, and poly-(L-DOPA) is adsorbed on the surface of Q235 carbon steel to form a protective film, which reduces the reaction of acidic solution and the surface of Q235 carbon steel and plays a role in corrosion protection[54]. However, it can be seen that there are still some pits on the surface of Q235 carbon steel under high magnification. It shows that when the concentration of poly-(L-DOPA) is high enough, the corrosion on the surface of Q235 carbon steel basically reaches equilibrium.

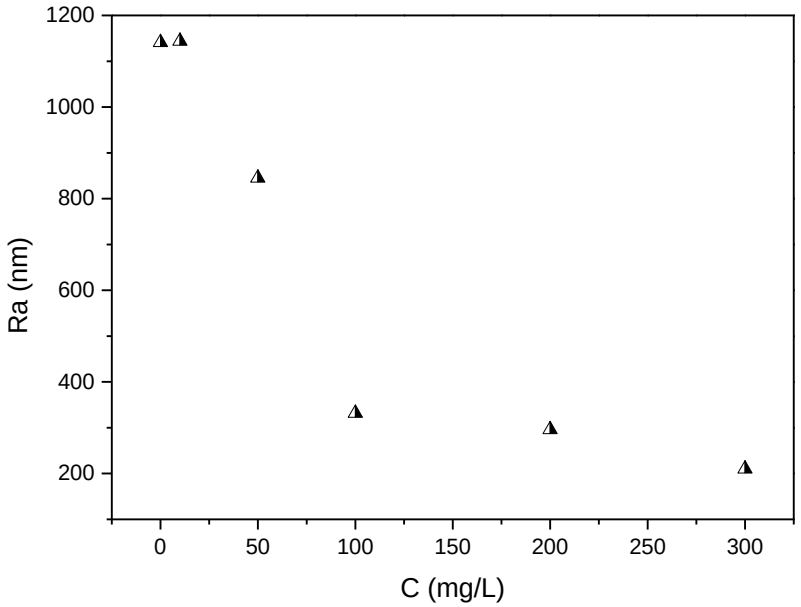

Figure 9. Ra after immersing Q235 carbon steel in 1 M HCl solution containing different concentrations of poly-(L-DOPA) for 12 hours.

Figure 8 provides a CLSM image of the sample. It can be seen that, compared with the polished Q235 carbon steel, the Q235 carbon steel immersed in 1 M HCl has a very rough surface, but with the addition of poly-(L-DOPA), the roughness of the sample has a significant decrease. Figure 9 shows the surface roughness (Ra) of Q235 carbon steel after soaking in 1 M HCl solution containing different concentrations of poly-(L-DOPA) for 12 hours. The Ra of the polished Q235 carbon steel is about 198 nm. After immersing Q235 carbon steel in a 1 M HCl solution containing 0 mg/L poly-(L-DOPA) and 10 mg/L poly-(L-DOPA), the roughness of the sample rose to 1141 nm and 1144 nm, respectively. When the concentration of poly-(L-DOPA) reaches 50 mg/L, the roughness of the sample drops to 845 nm. As the concentration of poly-(L-DOPA) increases to 100, 200, and 300 mg/L, the roughness of the sample decreases to 332, 296, and 210 nm, respectively. These data indicate that poly-(L-DOPA) has an effective corrosion inhibitory effect in acidic solutions[60].

4. CONCLUSION

We synthesized poly-(L-DOPA) through a simple self-polymerization method. Through systematic experiments and characterization, the results obtained summarized the following conclusions:

(1) The electrochemical results show that poly-(L-DOPA) has a significant inhibitory effect on the corrosion of Q235 carbon steel immersed in 1 M HCl. The inhibition efficiency increases with the increase of the concentration of poly-(L-DOPA) and the extension of the immersion time. When the concentration of poly-(L-DOPA) is 300 mg/L, the corrosion inhibition efficiency can reach 97%.

(2) The adsorption of poly-(L-DOPA) on the surface of Q235 carbon steel in 1 M HCl follows the Langmuir adsorption isotherm.

(3) Through SEM and CLSM observations, the inhibitory ability of poly-(L-DOPA) was confirmed, indicating that poly-(L-DOPA) can inhibit the corrosion of 1 M HCl by forming a dense protective film on the surface of Q235 carbon steel.

ACKNOWLEDGEMENTS
The authors gratefully appreciate financial support provided by the “One Hundred Talented People” of the Chinese Academy of Sciences (Y60707WR04).

References

1. M. Yadav, R. R. Sinha, T. K. Sarkar, I. Bahadur, E. E. Ebenso, *J. Mol. Liq.*, 212 (2015) 686.
2. R. Baskar, D. Kesavan, M. Gopiraman, K. Subramanian, *Prog. Org. Coat.*, 77 (2014) 836.
3. H. W. Liu, T. Y. Gu, Y. L. Lv, M. Asif, F. P. Xiong, G. A. Zhang, H. F. Liu, *Corros. Sci.*, 117 (2017) 24.
4. S. Pareek, D. Jain, S. Hussain, A. Biswas, R. Shrivastava, S. K. Parida, H. K. Kisan, H. Lgaz, I. M. Chung, D. Behera, *Chem. Eng. J.*, 358 (2019) 725.
5. P. Singh, M. Makowska-Janusik, P. Slovensky, M. A. Quraishi, *J. Mol. Liq.*, 220 (2016) 71.
6. Y. J. Qiang, S. T. Zhang, H. C. Zhao, B. C. Tian, L. P. Wang, *Corros. Sci.*, 161 (2019) 108193.
7. K. M. Ismail, *Electrochim. Acta*, 52 (2007) 7811.
8. H. Li, S. T. Zhang, B. C. Tan, Y. J. Qiang, W. P. Li, S. J. Chen, L. Guo, *J. Mol. Liq.*, 305 (2020) 112789
9. C. M. Rangel, J. D. Damborenea, A. I. D. Sá, M. H. Simplício, *Br. Corros. J.*, 27 (1992) 207.
10. D. Q. Zhang, Q. R. Cai, L. X. Gao, K.Y. Lee, *Corros. Sci.*, 50 (2008) 3615.
11. Y. J. Qiang, H. Li, X. J. Lan, *J. Mater. Sci. Technol.*, 52 (2020) 63.
12. N. Kovacevic, A. Kokalj, *Mater. Chem. Phys.*, 137 (2012) 331.
13. J. Zhang, G. M. Qiao, S. Q. Hu, Y. G. Yan, Z. J. Ren, L. J. Yu, *Corros. Sci.*, 53 (2011) 147.
14. S. Kaya, B. Tuzun, C. Kaya, I. B. Obot, *J. Taiwan Inst. Chem. Eng.*, 58 (2016) 528.
15. M. M. El-Naggar, *Corros. Sci.*, 49 (2007) 2226.
16. F. S. de Souza, A. Spinelli, *Corros. Sci.*, 51 (2009) 642.
17. V. S. Chary, K. C. Rajanna, G. Krishnaiah, P. Srinivas, *Catal. Sci. Technol.*, 6 (2016) 1430.
18. M. Yadav, T. K. Sarkar, T. Purkait, *J. Mol. Liq.*, 212 (2015) 731.
19. Y. G. Avdeev, Y. I. Kuznetsov, A. K. Buryak, *Corros. Sci.*, 69 (2013) 50.
20. X. W. Zheng, S. T. Zhang, W. P. Li, L. L. Yin, J. H. He, J. F. Wu, *Corros. Sci.*, 80 (2014) 383.
21. Z. Y. Hu, Y. B. Meng, X. M. Ma, H. L. Zhu, J. Li, C. Li, D. L. Cao, *Corros. Sci.*, 112 (2016) 563.

22. I. B. Obot, D. D. Macdonald, Z. M. Gasem, *Corros. Sci.*, 99 (2015) 1.
23. M. Mousavi, T. Baghgoli, *Corros. Sci.*, 105 (2016) 170.
24. P. Kannan, T. S. Rao, N. Rajendran, *J. Colloid Interface Sci.*, 512 (2018) 618.
25. Z. Z. Tasic, M. M. Antonijevic, M. B. Petrovic Mihajlovic, M. B. Radovanovic, *J. Mol. Liq.*, 219 (2016) 463.
26. G. L. F. Mendonça, S. N. Costa, V. N. Freire, P. N. S. Casciano, A. N. Correia, P. d. LimaNeto, *Corros. Sci.*, 115 (2017) 41.
27. Y. J. Qiang, S. T. Zhang, S. Yan, X. F. Zou, S. J. Chen, *Corros. Sci.*, 126 (2017) 295.
28. Z. Salarvand, M. Amirnasr, M. Talebian, K. Raeissi, S. Meghdadi, *Corros. Sci.*, 114 (2017) 133.
29. B. C. Tan, S. T. Zhang, Y. J. Qiang, L. Guo, L. Feng, C. H. Liao, Y. Xu, S. J. Chen, *J. Colloid Interface Sci.*, 526 (2018) 268.
30. M. Finšgar, *Corros. Sci.*, 72 (2013) 82.
31. F. Altaf, R. Qureshi, S. Ahmed, *J. Electroanal. Chem.*, 659 (2011) 134.
32. Y. He, R. R. Yang, Y. Q. Zhou, L. Ma, L. Zhang, Z. Chen, *Anti-Corros. Methods Mater.*, 63 (2016) 437.
33. L. Feng, S. T. Zhang, Y. Xu, Y. J. Qiang, S. J. Chen, *J. Mol. Liq.*, 286 (2019) 110893.
34. P. Singh, E. E. Ebenso, L. O. Olasunkanmi, I. B. Obot, M. A. Quraishi, *J. Phys. Chem. C*, 120 (2016) 3408.
35. B. C. Tan, S. T. Zhang, Y. J. Qiang, L. Feng, C. H. Liao, Y. Xu, S. J. Chen, *J. Mol. Liq.*, 248 (2017) 902.
36. S. A. Asipita, M. Ismail, M. Z. A. Majid, Z. A. Majid, C. Abdullah, J. Mirza, *J. Clean. Prod.*, 67 (2014) 139.
37. L. L. Liao, S. Mo, H. Q. Luo, N. B. Li, *J. Colloid Interf. Sci.*, 520 (2018) 41.
38. G. Ji, S. Anjum, S. Sundaram, R. Prakash, *Corros. Sci.*, 90 (2015) 107.
39. C. Kamal, M. G. Sethuraman, *Mater. Corros.*, 65 (2014) 846.
40. Y. J. Qiang, S. T. Zhang, B. C. Tan, S. J. Chen, *Corros. Sci.*, 133 (2018) 6.
41. P. Singh, A. Singh, M. A. Quraishi, E. Ebenso, *Int. J. Electrochem. Sci.*, 7 (2012) 8612.
42. R. S. Keri, S. A. Patil, *Biomed. Pharmacother.*, 68 (2014) 1161.
43. C. Verma, L. O. Olasunkanmi, E. E. Ebenso, M. A. Quraishi, J. Mol. Liq., 251 (2018) 100.
44. H. Lee, S. M. Dellatore, W. M. Miller, P. B. Messersmith, *Science*, 318 (2007) 426.
45. F. Yang, X. Y. Li, Z. D. Dai, T. Liu, W. R. Zheng, H. C. Zhao, L. P. Wang, *Int. J. Electrochem. Sci.*, 12 (2017) 7469.
46. E. E. Oguzie, C. K. Enenebeaku, C. O. Akalezi, S. C. Okoro, A. A. Ayuk, E. N. Ejike, *J. Colloid Interf. Sci.*, 349 (2010) 283.
47. A. Nalhe, E-O. Yssir, A. Bouyanzer, L. Majidi, J. Paolini, J. M. Desjobert, J. Costa, N. Chahboun, M. Zarrouk, B. Hammouti, *Orient. J. Chem.*,32 (2016) 1909.
48. J. W. Fu, Z. H. Chen, M. H. Wang, S. J. Liu, J. H. Zhang, J. N. Zhang, R. P. Han, Q. Xu, *Chem. Eng. J.*, 259 (2015) 53.
49. W. J. Barreto, S. Ponzoni, P. Sassi, *Spectroc. Acta Pt. A-Molec. Biomolec. Spectr.*, 55 (1999) 65.
50. Y. J. Qiang, S. T. Zhang, L. Guo, X. W. Zheng, B. Xiang, S. J. Chen, *Corros. Sci.*, 119 (2017) 68.
51. K. R. Ansari, M. A. Quraishi, A. Singh, *Corros. Sci.*, 79 (2014) 5.
52. T. Tüken, F. Demir, N. Kıcır, G. Sığırcık, M. Erbil, *Corros. Sci.*, 59 (2012) 110.
53. A. S. Algaber, E. M. El-Nemma, M. M. Saleh, *Mater. Chem. Phys.*, 86 (2004) 26.
54. P. Mourya, S. Banerjee, M. M. Singh, *Corros. Sci.*, 85 (2014) 352.
55. S. S. Abd El Rehim, S. M. Sayyah, M. M. El-Deeb, S. M. Kamal, R. E. Azooz, *Int. J. Ind. chem.*, 7 (2016) 39.
56. Z. Y. Hu, Y. B. Meng, X. M. Ma, H. L. Zhu, J. Li, C. Li, D. L. Cao, *Corros. Sci.*, 112 (2016) 563.
57. G. Sığırcık, T. Tüken, M. Erbil, *Corros. Sci.*, 102 (2016) 437.
58. Y. Tang, X. P. Guo, G. A. Zhang, *Corros. Sci.*, 118 (2017) 118.
59. R. A. Prabhu, T. V. Venkatesha, A. V. Shanbhag, G. M. Kulkarni, R. G. Kalkhambkar, *Corros. Sci.*,

50 (2008) 3356.
60. J. Telegdi, G. Luciano, S. Mahanty, T. Abohalkuma, *Mater. Corros.*, 67 (2016) 1027.